Simulating the last 1000 years with a 3d coupled model

Ulrich Cubasch++, Eduardo Zorita*, Jesus F. Gonzalez-Rouco+, Hans v. Storch* and Irina Fast++

* *GKSS Research Centre, 21502 Geesthacht, Germany*

+Dept de Astrofisica y Fisica de la Atmosfera, Universidad Complutense de Madrid, 28040 Madrid, Spain

++Metereologisches Institut, Freie Universität Berlin, Carl-Heinrich-Becker-Weg 6-10, 12165 Berlin, Germany

Abstract

A simulation of the climate of the last millennium with a state-of-the art ocean-atmosphere climate model, which has been forced with solar variability, volcanism and the change in anthropogenic greenhouse gases, shows global temperatures during the Little Ice Age of the order of 1 K colder than present. This is markedly colder than some accepted empirical reconstructions from proxy data. In this simulation temperature minima are reached in the Late Maunder Minimum, (around 1700 A.D.) and the Dalton Minimum (1820 A.D.), with global temperature about 1.2 K colder than today. The model also produces a Medieval Warm Period around 1100 A.D., with global temperatures approximately equal to present values.
A combination of model and tree-ring data leads to an improved temperature estimate for Northern Europe, but not for Southern Europe.

1. Introduction

A number of reconstructions of the climate of the past 500 - 1000 years have been published, which rely on data from various sources (tree rings, documentary evidence, ice cores, coral data, varved lake sediments, borehole data, etc.) as proxies using (multivariate) statistical calibration methods (Overpeck et al, 1997, Mann et al, 1998, 1999, 2000, Jones et al, 2001, Crowley and Lowery, 2000; Briffa et al, 2001, 2002, Esper et al, 2002; Luterbacher et al, 2002a,b, Mann and Jones, 2003; Luterbacher et al, 2004). More recently, the historic climate has been simulated in climate experiments using models of different complexity (Crowley, 2000; Bauer et al., 2003; Zorita et al., 2003), which are forced with the historical variations of solar flux, volcanism and greenhouse gases (Crowley, 2000, Solanki and Krivova, 2003, Etheridge et al, 1996, Blunier et al, 1995).

Nonclimatic "noise", potential nonlinearity and nonstationarity of proxy/climate relationships as well as seasonal biases, that are characteristic for proxy data (Jones and Mann, 2004), result in relatively large uncertainties of proxy-based climate reconstructions. Moreover currently available proxy data are regionally limited and the spatial coverage becomes increasingly sparse in more distant past.

The model data, on the other hand, have a global coverage, however, they depend on the quality of the model employed and on the prescribed external forcing, which, except for the last 30 years, is based on proxy data as well.

In the current paper a complex 3d coupled ocean-atmosphere model is employed to simulate the historic climate. After a description of the model and the experimental set-up (chapter2), the model results are analyzed and compared to observations (chapter 3). In chapter 4 a method to combine proxy data and model data and its application to data from the European region is introduced, followed by a summary (chapter 5).

2. The model and the experimental set-up

The climate model consists of the atmospheric model ECHAM4 with a horizontal resolution of 3.75 x 3.75 degrees and 19 vertical levels, 5 of them located in the stratosphere, coupled to the ocean model HOPE-G with a horizontal resolution of approx. 2.8x2.8 degrees with equator refinement and 20 vertical levels. The ocean and atmosphere models are coupled through flux adjustment to avoid climate drift in long climate simulations. This coupled model has been developed at the Max-Planck-Institute of Meteorology and it has been used in many studies of climate variability and climate change (Grötzner et al, 1998)

The model was driven by estimations of past variations of the solar constant, volcanic activity and concentrations of greenhouse gases (derived from air bubbles trapped in polar ice cores (Etheridge et al, 1996, Blunier et al, 1995)). Annual values of net radiative forcing due to solar variability and volcanic activity were estimated by Crowley (2000) from concentrations of ^{10}Be (a cosmogenic isotope), from historical observations of sun spots and acidity measurements in ice cores. In this simulation, they were translated to variations in an effective solar constant communicated to the climate model, represented by a global annual number, equally distributed over the solar spectrum, with no seasonal or geographical dependence. In the last two centuries

the solar component is very close to the Lean data (Lean et al, 1995). Changes in tropospheric sulphate aerosols and ozone concentrations have not been included.

Two experiments have been run: a first one starting in the year 1550 ("Columbus") and a second one starting in the year 1000 ("Erik").

3. The modelling results

The near-surface temperature

The external climate forcing and the simulated global annual near-surface air temperature (SAT), is represented in figure 1. The model simulates a temperature maximum around 1100 A.D., the Medieval Warm Period (MWP) (Jones et al, 2001), with temperatures very similar to the ones simulated for the present period. The existence of the MWP has been recently a matter of considerable debate, since proxy data have not yielded a consistent picture of its existence (Bradley et al, 2001, Broecker et al, 2001). In this simulation the MWP was a global phenomenon, probably caused by the maximum in solar activity in the 12th century. From 1300 A.D. global temperatures decrease and the simulation enters the so called Little Ice Age (LIA) lasting until about 1850 A.D (Jones et al, 2001). Temperatures in the LIA were about 1 K colder than today's values, the cooling peaking in the Late Maunder Minimum (Eady, 1976) (around 1700 A.D.) and the Dalton Minimum (Jones et al, 2001) (around 1820 A.D.), when simulated temperatures are about 0.25 K colder than the LIA mean. Subsequently, global temperatures start increasing almost continuously into the 20^{th} century until the end of the simulation. The simulated secular warming trend in the 20^{th} century is approached, but not surpassed, by warming trends around 1100 A.D. and in the 18^{th} century. The shorter simulation of the last 500 years with a slightly different model version yields similar results.

The simulated temperature evolution is at variance with the most accepted empirical reconstruction (Mann et al, 1999). The empirical reconstructions based on different proxy data have targeted different temperatures, depending on the sensitivity of the proxies used. Thus, the multi-proxy approach of Mann et al (1999), hereafter MBH99, represents a reconstruction of the annual Northern Hemisphere (NH) temperature, whereas the reconstruction by Esper et al. (2002), based on extratropical dendrochronological data, is probably more strongly biased towards the NH extratropical summer temperatures. Instead of re-scaling the reconstruction to a common framework (Briffa and Osborn, 2002), figure 2 shows these two not re-scaled reconstructions, together with the simulated NH annual temperature and the NH extratropical summer temperature. The discrepancies between reconstructions and simulations remain large, although up to 1600 A.D. the simulated values lie within the $2x\sigma$ errors of MBH99. The NH ECHO-G and MBH99 temperatures are reasonably correlated in the period 1000-1990 A.D., even when the long-term linear trends before and after 1900 A.D. are considered ($r=0.25$ at interannual timescales , 0.37 at decadal and longer timescales), but the amplitude of the variations is clearly different.

The ECHO simulations show a good agreement with a similar simulation of the last 500 hundred years, independently performed at the Hadley Center for Climate Research (Widmann and Tett, 2004). The latter model is not flux-adjusted, indicating that flux adjustment does not greatly distort the variability at long-time scales.

An assessment about the consistency of the model simulations and empirical reconstructions can be achieved by analysing the temperature evolutions in the 20th century, specially in the second half, when a global and complete climate data set of pseudo-observations- the National Centre for Environmental Prediction (NCEP) reanalysis (Kalnay, 1996) is available and solar output underwent strong variability (Lean et al, 1995). The analysis focuses on the NH temperature, which is arguably more reliable than the global mean. Figure 3a shows the NH annual SAT from the NCEP reanalysis together with the evolution of the solar constant. The correspondence between both in the period 1948-1990 A.D. strongly suggests that the solar forcing contributed to a large extent to the North Hemisphere cooling between 1950 A.D. and 1975 A.D. , the subsequent rapid warming (1975-1980 A.D.) and cooling (1980-1990) A.D.), a relationship also previously suggested from sea-surface-temperature data (White et al, 1997).

In the last decade greenhouse warming becomes dominant. The comparison with the Jones et al. (1999) instrumental data set leads to a similar conclusion (figure 3a). It is noted that ensemble simulations with the Hadley Centre model driven only by anthropogenic forcing deviate considerably from observations in this period (Stott et al, 2000).

The inclusion of the effect of volcanic activity would not have changed the overall picture, since in this period volcanic activity, as reflected in ice-core acidity measurements, was regularly distributed over time. The ECHO-G NH temperatures are depicted in Figure 3b. Both show a similar evolution, ruling out internal variability as cause for this behaviour, and suggesting that the model is able to simulate reasonably the effects of a varying solar output. The solar signal in the NH NCEP temperature at 30 mb height (not shown) is not as clear and agrees better than in the simulations, but figure 3b also suggests that a complex stratosphere model may not always be required (Haig, 1996), at least to simulate the NH temperature. Finally, figure 4c shows the MBH99 NH temperature, which in this period displays the smallest variability range.

Climate sensitivity

One can try to check the consistency of the different SAT data sets through a rough estimation of the sensitivity of the NH temperature to variations of the solar constant, although the climate sensitivity may be depend on the previous pathway and mean state of the climate (Senior et al, 2000; Meehl et al, 2002). By linearly detrending the temperature and solar constant in the 20th century, the presumably linear warming due to anthropogenic greenhouse gases and the linear increase in the solar constant may be filtered out. The correlation between detrended temperature and detrended solar constant should reflect the sensitivity of temperature to decadal variations of the solar constant, such as the ones of figure 3a. This correlation is represented in figure 5

for the NCEP reanalysis, the Jones et al. instrumental data, the longer ECHO-G simulation and the MBH99 reconstruction. The 20th century regression slopes yield a sensitivity of 0.13 K/(W/m^2) for the NCEP and Jones et al. instrumental data set, 0.11 K/(W/m^2) for ECHO-G temperature, and 0.08 K/(W/m^2) for the MBH99 reconstruction. Previous estimations based on empirical reconstructions yielded a close value of 0.12 K/(W/m^2) (Lean and Rind, 1999). A value of 0.13 K/W/m^2 corresponds to a sensitivity to net radiative forcing of about 0.75 K/W/m^2, assuming a fixed NH reflectivity of 30%, which is closed to the assumed sensitivity to changes in greenhouse gas forcing (IPCC, 2001) and model simulations driven by solar changes (Cubasch et al, 1997). This sensitivity would explain about 0.2K of the NH warming in 1970-1999, approximately one third of the observed NH warming. This is close to a value of 40% estimated from simulations with other models driven by solar forcing alone (Cubasch et al, 1997)

The same sensitivity analysis has been carried out for the ECHO-G simulation and the MBH99 reconstruction in the period 1600-1900 A.D. In this period, greenhouse gases variations should have played a minor role, so that no other external trends are to be expected. This analysis yields a sensitivity of 0.16K/(W/m^2) for ECHO-G and 0.02K/(W/m^2) for MBH99. The data from this period are also depicted in figure 4. The sensitivity of the ECHO-G model seems to have been larger in the previous centuries.

Uncertainties in this rough estimate, the different pathway and mean climate in the LIA (Senior et al, 2000; Mehl et al, 2002), or the presence of stronger volcanic activity could contribute to explain this change. However, the sensitivity derived from the MBH99 reconstruction in the previous centuries is a factor 4 smaller than in the 20th century, possibly indicating that the reconstructions of the solar constant and the empirical temperature reconstructions in the previous centuries are not consistent with their behaviour in the 20th century.

4. Synthesis of model and proxy data

As the proxy data become more and more sparse the further one goes back into the past (figure 5), one can try to substitute the missing proxy information by model data. An approach for combining tree-ring data from Europe and the historical climate model simulations is presented in the next chapter.

4.1 Methodology and data

The main idea of the approach is the application of statistical climate field reconstruction methods to a *composed* network of proxy and model derived *pseudo-proxy* data (figure 6). Different options are open with regard to the processing and geographical location of pseudo-proxy data, as well as weighting of proxy and pseudo-proxy data.

Following dataset were used to reconstruct the climate over Europe:

(1) The instrumental dataset CRUTEM2v of gridded monthly mean surface air temperature anomalies relative to the 1961-1990 period (Jones et al, 1999, Jones and Moberg, 2003). The data are available on a 5°x5° grid from 1851, although with some notable gaps. 66 grid boxes form the reconstruction area (figure 5a). This compilation of instrumental measurements was chosen to allow for a consistency with other existing temperature reconstructions (e.g. Mann et al, 1998, Briffa et al, 2002).

(2) Gridded measurements of the tree ring density (MLD = Maximum Latewood Density) from the „Schweingruber"-network (Briffa et al, 2001, 2002). The spatial distribution of time-varying data is shown in figure 5a, the temporal changes of availability are presented in figure 5b. In the period of maximal data density (1858-1976) 34 grid boxes of the area are covered with proxy data. Only 7 of these proxy time series are starting at around 1400. An adjustment procedure was applied to the tree-ring data to restore the low-frequency climate variability removed during the standardization.

(3) Temperature fields from above described historical climate model simulations "Columbus" and "Erik".

For calibration of proxy networks against instrumental data a partial-least square (PLS)-regression approach (Martens and Nes, 1989) was used. The method is based on the simultaneous decomposition of predictors and predictands in order to extract components, which explain as much as possible covariance between them. The first few of the extracted components (also called latent vectors) are used in the regression equations instead of the full set of predictors and predictands.
Following to the results of Briffa et al. (2002) MLD network was calibrated against the mean April-September instrumental temperature anomalies. The temporal calibration is based on data from time interval 1897-1976 (calibration period), which is characterized through a better spatial coverage with the measurements. The first 46 years of the instrumental period (1851-1897) have been reserved to validate the derived statistical relationships with independent data.

Monthly averaged simulated temperature fields from "Columbus" and "Erik" runs were interpolated to the observational grid to construct the appropriate pseudo-proxy data from model output. Thereafter the April-September mean temperature anomalies relative to the simulated 1961-1990 means were calculated. Finally the model data were sub-sampled to mimic the time-varying spatial distribution of tree-ring data and averaged across the both simulations.
To take into account a somewhat different nature of proxy and pseudo-proxy data, the PLS-regression was extended to the so-called tri-PLS Regression (Bro, 1998). For this purpose proxies and model derived pseudo-proxies were arranged in a 3-dimensional data matrix.

Prior to the analysis, predictors and predictands were column-wise standardized using corresponding calibration period mean and standard deviation. Due to the changing number of proxy data series during the considered time span the calibration procedure had to be performed several times. In all calibration models the first 4 latent vectors have been retained, which explain 32 to 52% (depending on the number of available

proxies) of the interannual temperature variations during the calibration period.

To assess the reconstructive skill of derived statistical models two following statistics were used (*Cook and Kairiukstis, 1990*):

(1) Reduction of error (RE), defined as

$$RE = 1 - \sum_{i=1}^{n} (obs_i - rec_i)^2 \Big/ \sum_{i=1}^{n} (obs_i - \overline{obs}^{cal})^2 ;$$

(2) Coefficient of efficiency (CE), defined as

$$CE = 1 - \sum_{i=1}^{n} (obs_i - rec_i)^2 \Big/ \sum_{i=1}^{n} (obs_i - \overline{obs}^{val})^2 \ ,$$

where rec_i are the reconstructed values, obs_i are the instrumental measurements and $\overline{obs}$ is the mean over calibration (validation) period. RE = 0 (CE = 0) defines the performance of a simple "climatologic" model, in which a whole series is assigned to its calibration (validation) period mean temperatures. Negative values indicate a unusable reconstruction.
We calculated this statistics for each grid box as well as for 3 regional averaged series: Europe (whole reconstruction area), Northern Europe (north of 53°N) and Southern Europe (south of 53°N).

4.2 Result

Figure 7 shows regionally averaged reconstructed temperatures anomalies for pure tree-ring based reconstruction (TR) and for joint tree-ring and model reconstruction (TRM). In the Northern Europe one can see an improvement, which is also reflected in the objective reconstruction skill score (RE) (figure 8). In the Southern Europe the model information rather leads to a degradation of reconstructive skill. The distinct difference in the behaviour of southern and northern Europe might indicate a systematic problem either in the tree-rings (are trees responding different to the climate change in different latitudes) or model problems, mainly orography.

A challenging issue is an assessment of the added value of model information comparing to the pure proxy-based reconstruction. This can be addressed via comparison with independent climate reconstructions, which rely on not used proxy data. Another possibility constitutes a form of Monte-Carlo simulation. In order to construct ranges of "by chance changes" a large number of "random" pseudo-proxy time series can be generated from an unforced control model simulation (e.g. by shifting the begin of time series and appending of the cut-off segment at the end or by permutation of years) and used in the above described calibration procedure.
In the case of the improvement of proxy-based reconstruction by model information, which lies beyond the uncertainty ranges from Monte-Carlo simulations, one gains confidence in the consistency of model, proxy and instrumental data.

5. Summary

The discrepancies between model simulation and empirical reconstructions are discussed in terms of the climate sensitivity to changes in the solar constant. We find that whereas the model response to changes is roughly constant along the simulation and agrees with the sensitivity derived from instrumental data, the empirical reconstructions show a lower sensitivity in the 20th century, and a much lower one in the past centuries, thus pointing to potential inconsistencies between the reconstructed temperature and solar constant.

It has been tried to use the model data to fill gaps in the proxy-data records. This produces an improved temperature curve for northern Europe. Problems, however arise in southern Europe.

References

Bauer, E., Claussen, M., Brovkin, V. & Huenerbein, A. Assessing climate forcings of the earth system for the past millennium, *Geophys. Res. Lett.* 30 (6), doi: 10.1029/2002GL016639, (2003).

Blunier , T., Chappellaz, J.A., Schwander, J. , Stauffer, B. & Raynaud, D. Variations in atmospheric methane concentration during the Holocene epoch. *Nature* **374**, 46-49 (1995)

Bradley, S., Briffa, R.K, Crowley,T.J., Hughes, M.K., Jones,, P.D. & Mann M.E. The scope of Medieval warming *Science* **292**, 2011-2012 (2001).

Briffa, K.R. & Osborn, T.J. Blowing hot and cold. *Science* **295,** 2227-2228 (2002).

Briffa, K.R., Osborn, T.J., Schweingruber, F.H., Harris,I.C., Jones, P.D., Shiyatov, S.G. & Vaganov, E.A. Low-frequency temperature variations from a northern tree ring density network. *J. Geophys. Res*. **106**, 2929–2941 (2001).

Briffa, K.R., Osborn, T.J., Schweingruber, F.H., Jones, P.D., Shiyatov, S.G. & Vaganov, E.A. Tree-ring width and density data around the Northern Hemisphere: Part 1, local and regional climate signals. *The Holocene* **12(6)**, 737-757 (2002).

Bro, R. Multi-way analysis in the food industry: Models, algorithms, and applications. PhD thesis, Royal Veterinary and Agricultural University, Denmark (1998).

Broecker, W.S. Was the Medieval Warm Period Global?. *Science* **291**, 1497-1499 (2001).

Cook, E.R. & Kairiukstis, L.A. (eds.) (1990), Methods of Dendrochronology: Applications in the Environmental Sciences, Kluwer Acad., Norwell, Mass.

Crowley, T.J . Causes of climate change over the past 1000 years. *Science* **289**, 270-277 (2000).

Crowley, T. J. & Lowery, T.S. How warm was the Medieval Warm Period? A comment on 'Man-made versus natural climate change' *Ambio* **39**, 51–54 (2000).

Cubasch , U. , Hegerl ,G.C., Voss, R., Waszkewitz, J. & Crowley, T.C. Simulation with an O-AGCM of the influence of variations of the solar constant on the global climate. *Clim. Dyn*. **13**, 757-767 (1997).

Eady, J.A. The Maunder Minimum. *Science* **192**, 1189-1202 (1976).

Etheridge, D. , Steele, L.P., Langenfelds, R.L., Francey, R.J., Barnola, J.M. & Morgan V.I. Natural and anthropogenic changes in atmospheric CO_2 over the last 1000 years from air in Antarctic ice and firn. *J. Geophys. Res.* **101**, 4115-4128 (1996).

Esper, J., Cook, E.R. & Schweingruber, F.H. Low-frequency signals in long tree-ring chronologies for reconstructing past temperature variability. *Science* **295**, 2250-2253 (2002) .

Goertzner, A., Latif, M., Barnett, T.P.A decadal climate cycle in the North Atlantic Ocean as simulated by the ECHO coupled. *J. Clim*. **11**, 831-847 (1998).

Haig, D.H. The impact of solar variability on climate. *Science* **272**, 981-984 (1996).

IPCC 2001. Houghton J.T. *et al.* (eds) *Climate Change 2001: The scientific basis* Cambridge Univ. Press, Cambridge (2001).

Jones, P.D. & Mann, M.E. Climate over past millennia. *Reviews of Geophysics*, **42**, doi:10.1029/2003RG000143 (2004).

Jones, P.D. & Moberg, A. Hemispheric and large-scale surface air temperature variations: An extensive revision and an update to 2001. *J. Clim*. **16**, 206–223 (2003).

Jones, P.D., New, M., Parker, D.E., Martin, S. & Rigor I.G. Surface air temperature and its changes over the past 150 years. *Rev. Geophys* . **37**, 173-199 (1999).

Jones, P.D., Osborn, T.J. & Briffa, K.R. The evolution of climate over the last millennium. *Science* **292,** 662-667 (2001).

Kalnay, E. et al. The NCEP/NCAR 40-year Reanalysis Project. *Bull. Amer. Meteor. Soc*. **77**, 437-471 (1996).

Lean ,J. , Beer, J. & Bradley, R. Reconstructions of solar irradiance since 1610-implications for climate change. *Geophys. Res. Lett.* **22,** 3195-3198 (1995).

Lean ,J. , Beer, J. & Bradley, R. Reconstructions of solar irradiance since 1610-implications for climate change. *Geophys. Res. Lett.* **22,** 3195-3198 (1995).

Lean, J. & Rind, D. Evaluating sun-climate relationships since the Little Ice Age. *J. Atmos. Sol.-Terr. Phys*. **61**, 25-36 (1999).

Mann, M.E. & Jones, P.D. Global surface temperatures over the past two millennia *Geophys. Res. Lett.* **30(15)** CLM 5-1 - 5-4 (2003).

Mann, M.E., Bradley, R.S., & Hughes, M.K. Global-scale temperature patterns and climate forcing over the past six centuries. *Nature* **392**, 779-787 (1998).

Mann, M.E., Bradley, R.S., & Hughes, M.K. Northern Hemisphere Temperatures During the Past Millennium: Inferences, Uncertainties, and Limitations. *Geophys. Res. Lett.*, **26,** 759-762 (1999).

Mann, M. E., Gille, E., Overpeck, J., Gross, W., Bradley, R.S., Keimig, F.T & Hughes, M.K. Global temperature patterns in past centuries: An interactive presentation, *Earth Interact*., **4** (2000). (Available at http://EarthInteractions.org)

Luterbacher, J. et al. Extending North Atlantic Oscillation reconstructions back to 1500. Atmos. Sci. Lett. 2, 114–124 (2002a).

Luterbacher, J., Xoplaki, E., Dietrich, D., Rickli, R., Jacobeit, J., Beck, C., Gyalistras, D., Schmutz, C. & Wanner, H. Reconstruction of sea level pressure fields over the eastern North Atlantic and Europe back to 1500. *Clim. Dyn.* **18**, 545–561 (2002b).

Luterbacher, J., Dietrich, D., Xoplaki, E., Grosjean, M. & Wanner, H. European seasonal and annual temperature variability, trends and extremes since 1500, *Science* **303**, 1499-1503 (2004).

Martens, H. & Nes, T. Multivariate Calibration, John Wiley, Chichester (1989).

Meehl, G., Washington ,W.M., Wigley, T.M.L., Alabaster,, J. & Dai A. Solar and greenhouse gas forcing and climate response in the twentieth century. *J. Climate* **16**, 426-443 (2002).

Overpeck, J., Hughen, K., Hardy, D., Bradley, R., Case, R., Douglas, M., Finney, B., Gajewski, K., Jacoby, G., Jennings, A., Lamoureux, S., Lasca, A., MacDonald, G., Moore, J., Retelle, M., Smith, S., Wolfe, A. & Zielinski, G. Arctic environmental change of the last four centuries, *Science* **278**, 1251–1256 (1997).

Senior, C.A. & Mitchell, J.F.B. The time-dependence of climate sensitivity. *Geophys. Res. Lett.* **27**, 2685 - 2688 (2000).

Solanki, S. K & Krivova, N.A. Can solar variability explain global warming since 1970?, *J. Geophys. Res.* **108(A5)**, 1200 (2003).

Stott, P. A. , Tett, S.F. B, Jones, G.S., Allen, M.R., Mitchell, J.F.B. &Jenkins, G.J . External control of 20th century temperature variations by natural and anthropogenic forcings. *Science* **15**, 2133-2137 (2000).

White ,W.B., Lean, J., Cayan, D.R.& Dettinger, M.D. Response of global upper ocean temperature to changing solar irradiance. *J. Geophys. Res.* **102**, 3255-3266 (1997).

Widmann, M. & Tett, S.F.B. Simulating the climate of the Last Millennium. IGBP Newsletter, 56. 10-13 (2004)

Zorita, E., von Storch, H., González-Rouco, F.J., Cubasch, U., Legutke, S., Fischer-Bruns, I. & Schlese U. Simulation of the climate of the last five centuries. *GKSS report*, **2003/12** (2003).

A**cknowledgements.** The authors thank S. Legutke and U. Schlese for providing the model and their support in running the simulations. The use of Crowley's, Jones et al. data and data from the NCEP is greatly acknowledged. This work was performed in the frame of the German programme DEKLIM , project REN2000-0786CLI from the Spanish CICYT and the EU project SOAP. Dennis Bray provided editorial assistance.

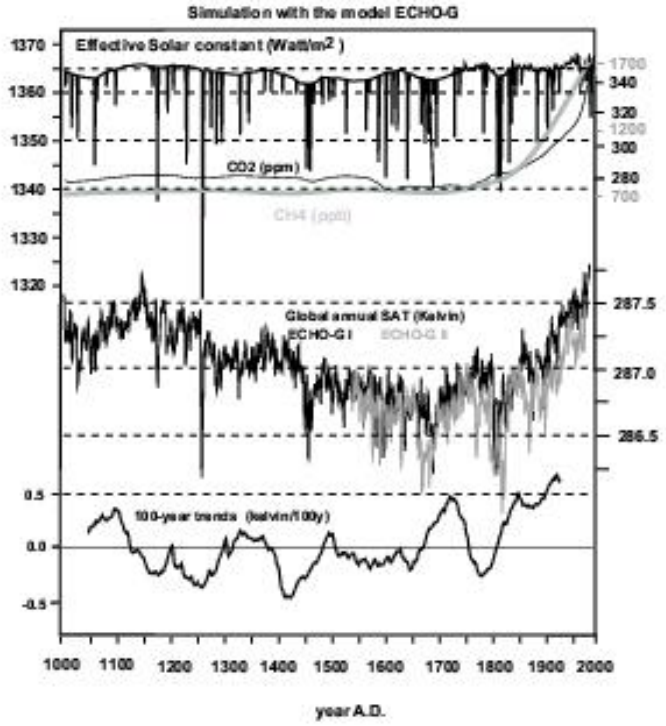

Figure 1: External forcing (effective solar constant and greenhouse gas concentration used to drive the climate model ECHO-G; the simulated global annual surface air temperature (SAT) for two ECHO-G simulations and the running 100-year SAT trends for the 1000-year simulation. The spikes in the effective solar constant represent the effect of volcanic aerosols on the radiative forcing. In 1258-9 A.D. an eruption of unknown location, recorded in the acidity measurements of ice cores, causes a temperature drop of about 1K.

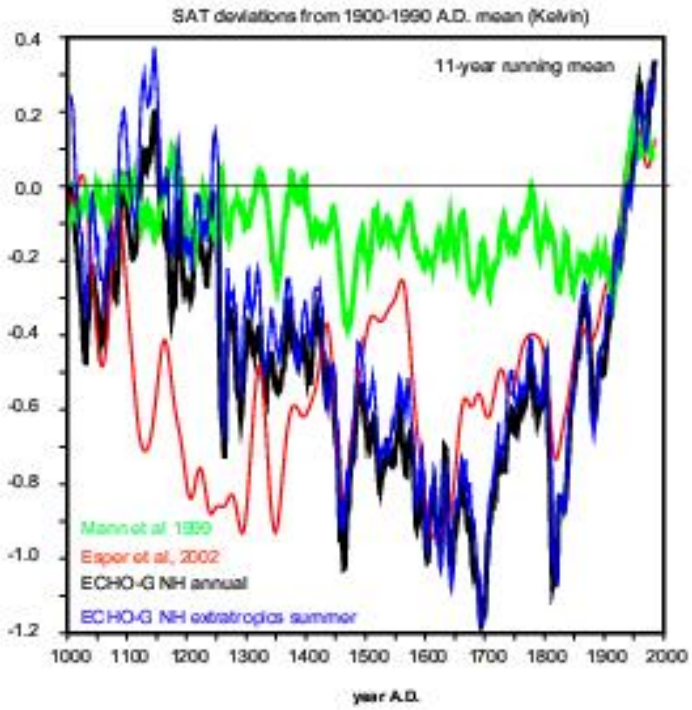

Figure 2: Simulated annual and summer extratropical North Hemisphere SAT deviations compared to two empirical reconstructions in the last millennium by Mann et al (2000) and Esper et al (2002).

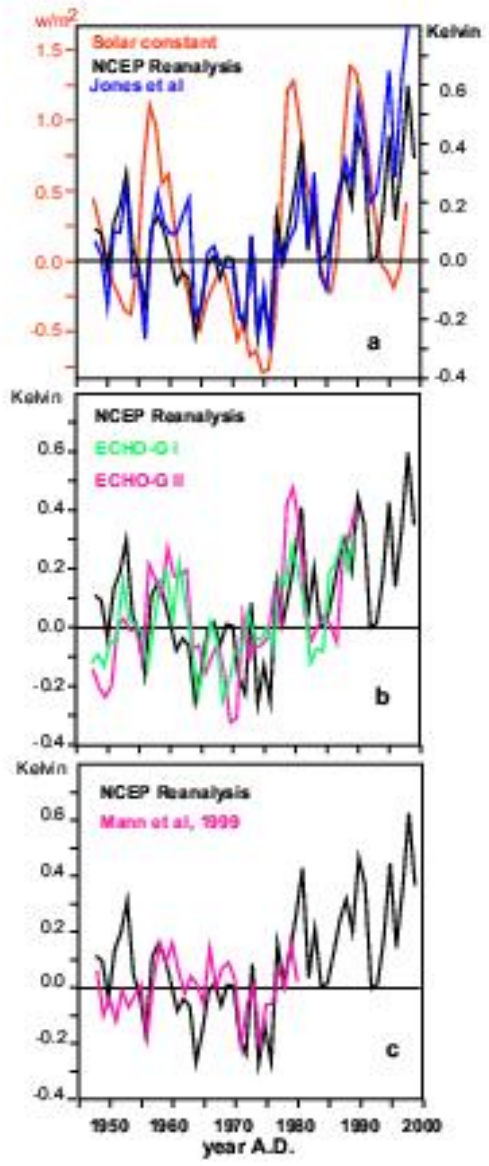

Figure 3: Comparison of different North Hemisphere surface temperature average in the period 1900-1999 from the NCEP Reanalysis, the ECHO-G simulations, the Jones et al. (2001) instrumental data set and the MBH99 reconstructions. The evolution of the solar constant as used in the ECHO simulations (derived from the Crowley (2000)) is also included in the upper-left panel. Data are deviations from the 1948-1980 mean.

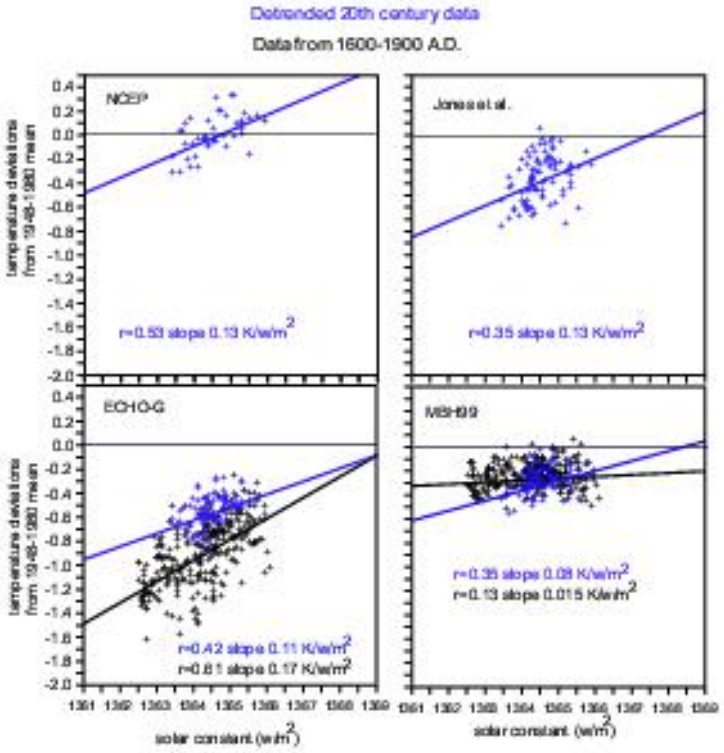

Figure 4: Scatter diagrams of annual solar constant, derived from Crowley (2000), and the North Hemisphere annual temperature deviations from the 1948-1990 mean for the NCEP data set, the Jones et al. (1999) instrumental data, the ECHO-G simulations and the MBH99 reconstruction. Black dots include data from the period 1600-1900 A.D, blue dots include linearly detrended data from 1900-1990 A.D. The correlation coefficients and the regression slopes are indicated.

(a)

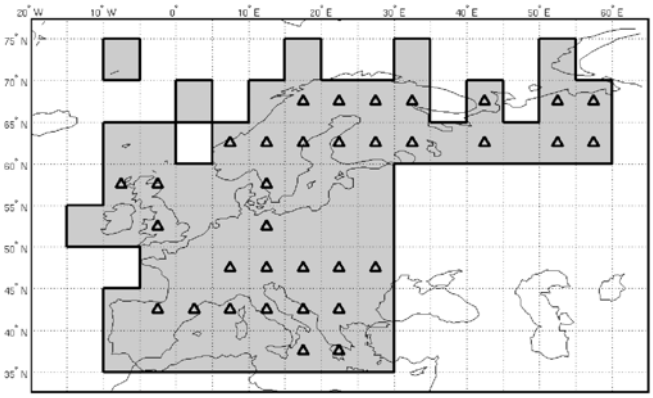

(b)

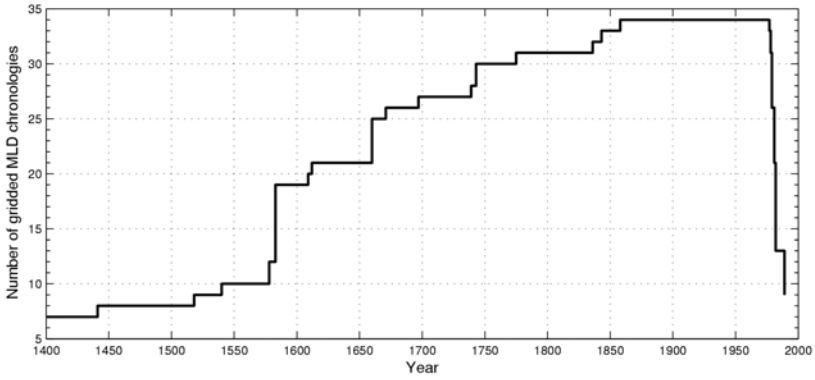

Figure 5: (a) European reconstruction domain (shaded) and location of gridded tree-ring data (triangles, maximal coverage); (b) temporal changes of the number of available tree-ring data.

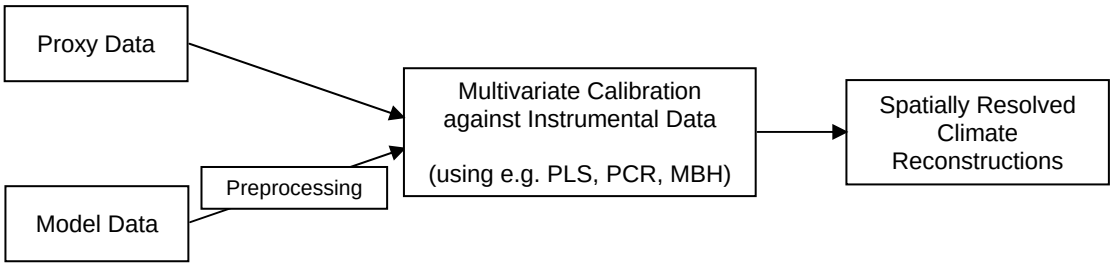

Figure 6: Schematic illustration of approach aimed to combine proxy and model information to reconstruct climate variability.

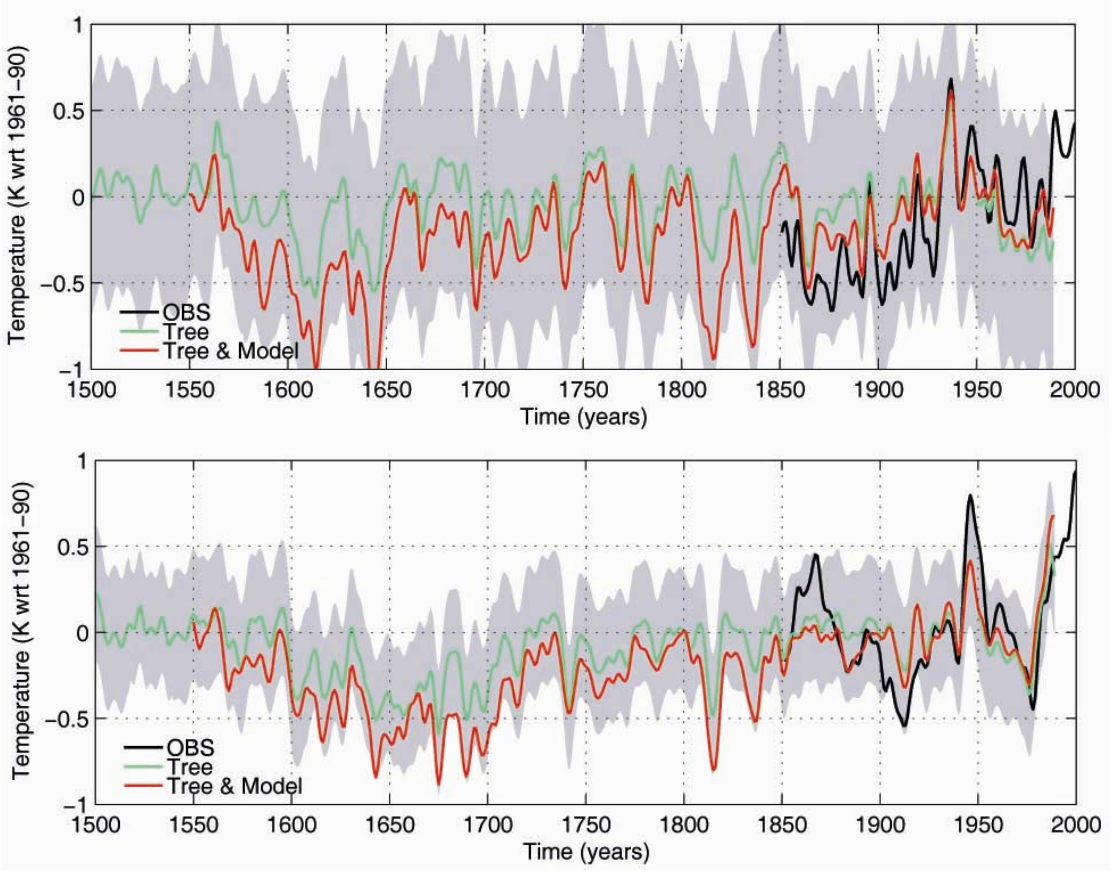

Figure 7: Reconstructed (TR: green, TRM: red) and instrumental (black) mean April-September temperature anomalies (wrt 1961-1990 mean) for Northern Europe (top) and Southern Europe (bottom) over the last 500 years. The uncertainty range of the tree-ring based reconstruction (estimated as doubled standard error for validation period) is shaded.

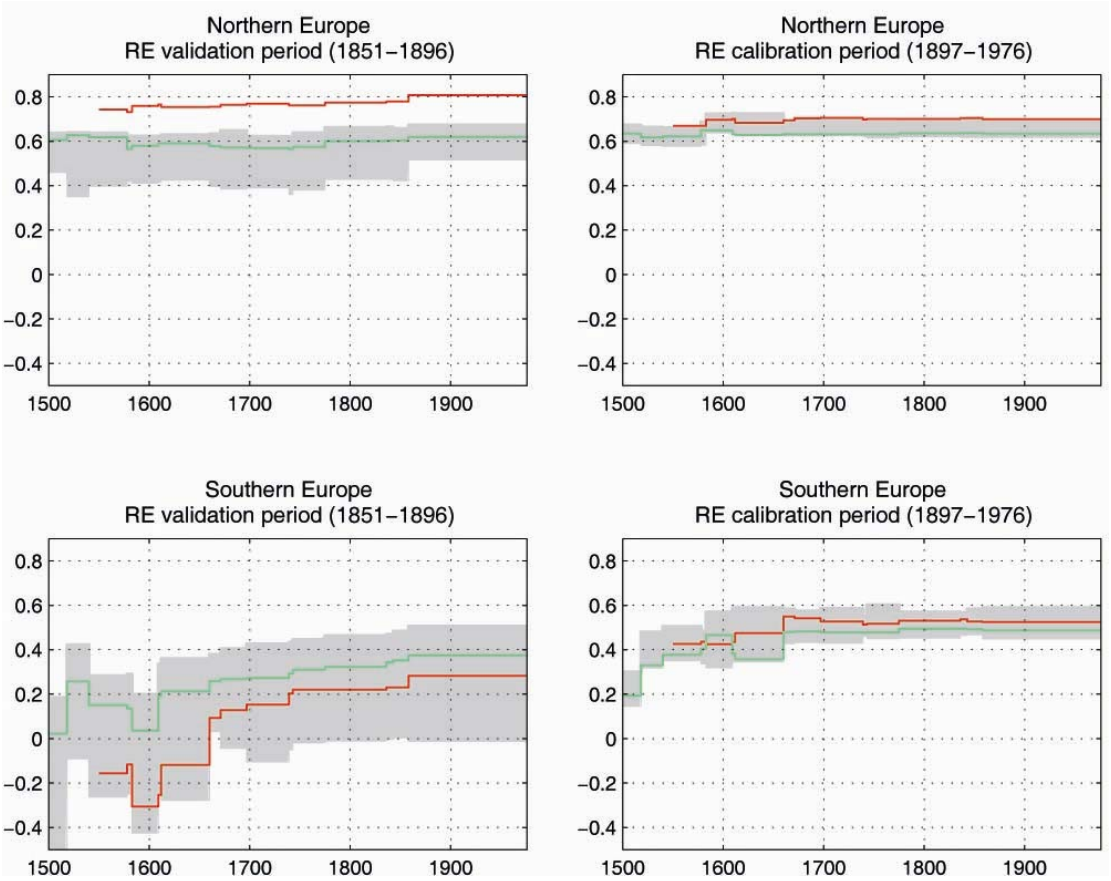

Figure 8: Reduction of error (RE) for Northern Europe (top) and Southern Europe (bottom) averaged temperature anomalies for pure tree-ring based reconstruction (green), and for tree-ring and model based reconstruction (red). The shaded uncertainty range is estimated by means of Monte-Carlo simulations, which use pseudo-proxies derived from an externally unforced climate simulation.